

Dynamics in Rhodopsin

Judith Klein-Seetharaman*[a]

KEYWORDS:

activation mechanism • conformation analysis • helical structures • G-protein-coupled receptors • membrane proteins

1. Introduction

Rhodopsin is the mammalian dim-light photoreceptor molecule and the prototypic member of the G-protein-coupled receptor (GPCR) family, the largest known family of cell surface receptors.^[1] GPCRs transduce signals from the exterior to the interior of the cell in response to diverse stimuli such as hormones, neurotransmitters, odorant molecules, light, among others. GPCRs share a common structural motif, a bundle of seven transmembrane (TM) helices, which divides the proteins into cytoplasmic (CP), TM, and extracellular (EC) domains (shown for rhodopsin in Figure 1). The first step in the signal transduction

the CP domain that result in formation of the activated state. This activated state is recognized by the G protein transducin. The conserved seven-helical motif and related structural features led to the hypothesis that similar helix movements occur in all GPCRs in response to ligand-induced activation.^[1] Therefore, the mechanism of GPCR activation is believed to be fundamentally the same for all GPCRs. An understanding of the mechanism of signal transduction by GPCRs is linked to the precise molecular description of the conformational change that occurs in rhodopsin upon light-induced activation and in GPCRs in general upon ligand binding. As a result of the prototypical character of rhodopsin, mechanistic studies have focused on, 1) the tertiary

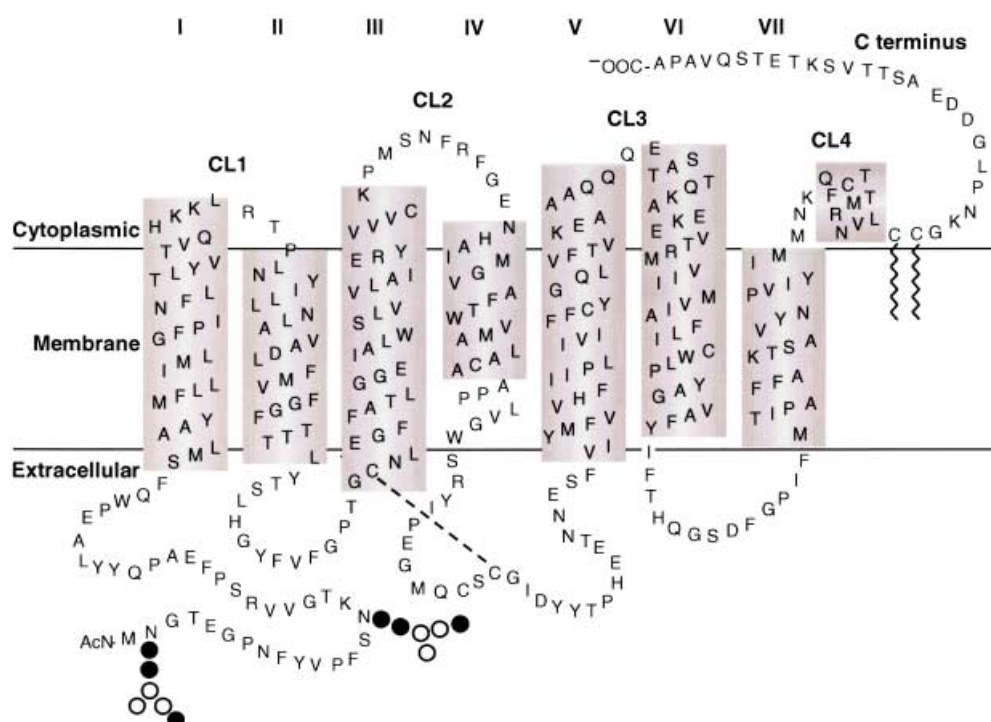


Figure 1. Secondary structure model of bovine rhodopsin showing intracellular (CP), TM, and EC (intradiscal in rhodopsin, extracellular in other GPCRs) domains. CP loops are marked CL1–CL4. The TM helices are designated I–VII. The conserved disulfide bond in rhodopsin is between Cys110 and Cys187. Cysteine residues 322 and 323 are palmitoylated. Approximate CP and TM boundaries are shown by horizontal lines.

mechanism of a GPCR is the binding of ligands (agonists) specific to each receptor. In the special case of rhodopsin, light induces isomerization of a covalently attached chromophore ligand, 11-*cis*-retinal (a vitamin A derivative), to all-*trans*-retinal. This isomerization activates the receptor by causing movements of the TM helices, which, in turn, induce conformational changes in

[a] Prof. J. Klein-Seetharaman
Department of Pharmacology
University of Pittsburgh School of Medicine
E1355 Biomedical Science Tower
Pittsburgh, PA 15261 (USA)
Fax: (+1) 412-648-1945
E-mail: jks33@pitt.edu

structures of rhodopsin in the different conformational states, and 2) the dynamic properties of these conformational states. The three-dimensional atomic model of dark-state rhodopsin has been elucidated by X-ray crystallography^[2] and its relation to inferences about structure based on previous biochemical and biophysical studies of rhodopsin and of other GPCRs has been discussed in recent reviews.^[3–5] Although the crystal structure corresponds to the dark-state rhodopsin, when this structure was taken together with the conclusions from other studies^[6–13] about the conformational changes that accompany light-induced activation, a low-resolution picture of such activation emerged. The perturbation of the seven-helical TM bundle by light-induced retinal isomerization results in an opening of the helical bundle towards the CP ends of the helices involving predominantly helices III, VI, and VII. This is consistent with the experimentally observed increases in the distances between the CP loops that connect the helices upon light-induced activation, most notably between CL1 and CL4,^[14, 15] and CL2 and CL3.^[8] The resulting cleft in the center of the helical bundle is believed to provide space for the interaction with transducin. Previous recent reviews of the mechanism of rhodopsin activation have focused on the structure of rhodopsin in the dark and the structural changes that accompany light-induced activation.^[3–5] The present review aims to summarize current insight into the dynamic properties of the dark-state structure of rhodopsin in solution since these properties are important for understanding the transition between the dark-state and light-activated conformations.

2. Dynamic Properties of the Rhodopsin Dark-State Crystals

The crystal structure of rhodopsin is a static “snapshot” of the dark-adapted conformation of rhodopsin. However, crystals do contain some dynamic information in the form of temperature or B factors that report on temporal and spatial displacements in the positions of the atoms. The B factors of the atoms in the rhodopsin crystal dimer are shown in Figure 2. There is large variation in B factors at the different positions along the sequence, with greatly increased disorder in loop regions. This effect is also observed for other membrane proteins for which crystal structures have been determined, which include the other 7-helical TM proteins bacteriorhodopsin^[16, 17] and sensory rhodopsin.^[18] However, the B factors along the rhodopsin sequence are different from those along the bacteriorhodopsin and sensory rhodopsin sequences in that the disorder in rhodopsin is disproportionately large for CP

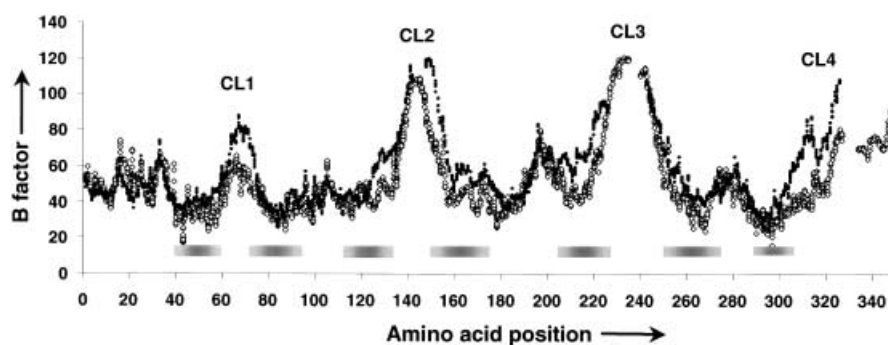


Figure 2. B factors along the rhodopsin sequences for both dimers reported in ref. [2]. The positions of the TM helices (shading) and CP loops (see Figure 1) are indicated. \diamond = crystal 1, \bullet = crystal 2.

extramembrane regions as compared to EC extramembrane regions. Thus, the CP loops CL2, CL3, and CL4 (which includes the C-terminal end), and to a lesser extent CL1, as well as the adjacent CP ends of the helices, are very disordered as compared to the rest of the molecule in the static crystal structure (Figure 2). This observation suggests the presence of a gradient in mobility along the TM domain from the EC ends of the helices towards the CP ends, with maximum mobility in the CP loops that connect the helices.

3. Qualitative Reporters of Side-Chain Mobility and Structure of the Cytoplasmic Loop Regions in Solution

The structure and dynamics of the CP loop regions and CP ends of the helices of rhodopsin in solution have been investigated in a large number of studies by using a combination of cysteine mutagenesis followed by biochemical and biophysical studies of the cysteine mutants. Figure 3 shows the residues on the CP side of the molecule that were replaced, one at a time, by cysteine. The unique chemistry of the cysteine sulfhydryl group allows specific derivatization of reactive and accessible cysteine residues with biophysical probes. Dark-state, wild-type rhodopsin contains two reactive cysteine residues, Cys140 and Cys316. These cysteine residues were replaced by serine residues in the cysteine mutants to avoid ambiguity. The other cysteine residues in rhodopsin (palmitoylation sites, TM and EC cysteine residues;

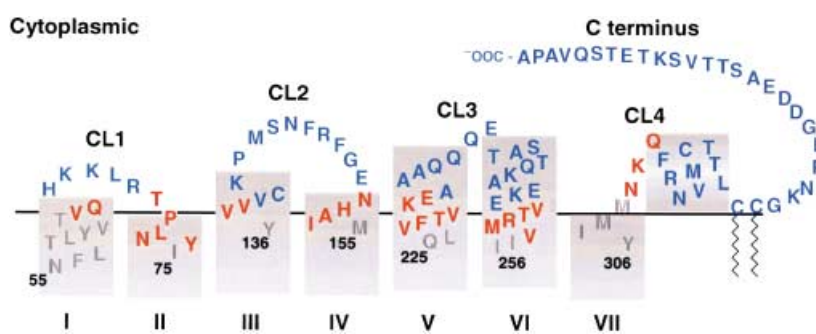


Figure 3. Secondary structure model of the CP ends of helices and the interconnecting sequences CL1–CL4, as in Figure 1. The residues located in the membrane and in the EC domain that were not studied by cysteine mutagenesis are omitted in this figure.

see Figure 1) are not reactive in the dark, and were therefore not replaced. Figure 4 lists some of the biophysical probes that have been used in the study of structure and dynamics in rhodopsin. Rhodopsin carrying a free sulfhydryl group reacts with 4,4'-dithiodipyridine to form the dipyridinyl derivative **1** shown in Figure 4.^[19] The rate of this reaction is very sensitive to the accessibility of the cysteine; cysteine residues buried in the micelle or protein interior are entirely unreactive and cysteine residues exposed in the fully accessible aqueous portion of the CP domain react instantly.^[9] The positions of these exposed cysteine residues correspond well with those identified by collision of paramagnetic agents with spin-labeled derivative **3**.^[20] The thiopyridinyl derivative of rhodopsin, **1**, is reactive towards free sulfhydryl reagents by way of disulfide exchange. The rate of this exchange is an extremely sensitive probe for tertiary structure and has been used to prove the presence of light-induced conformational motions that result in distinct tertiary structure changes,^[9] even where traditional methods suggest the magnitude of conformational change to be small.^[20] The disulfide exchange reaction of thiopyridinyl rhodopsin (**1**) with sulfhydryl reagents has practical value in that the nature of the sulfhydryl reagent can be chosen relatively freely and the reaction thereby presents a general scheme for derivatization with reporter probes of cysteine groups on proteins for which no reactive derivatives exist. For example, it was possible to derivatize rhodopsin with the trifluoroethylthiol group to give molecular entity **2** (Figure 4), which enabled ¹⁹F NMR spectroscopy applications.^[21] The position and width of ¹⁹F NMR spectroscopy signals are indicators of chemical environment and mobility^[22] and are therefore sensitive to light-induced conformational changes in rhodopsin.^[21]

The most direct indicators of the mobility of cysteine-derivatized rhodopsin are provided by EPR spin labels, as in **3** and **4** (Figure 4). The EPR spectrum of cysteine derivative **3** represents a mixture of side-chain and backbone motion, while that of **4** is dominated by motion of the side chain alone.^[23] Figure 5 shows a summary of the results obtained from EPR spectroscopy of rhodopsin derivative **3**.^[6, 7, 20, 24] Residues at the CP ends of helices are placed on helical wheels. As one can see in

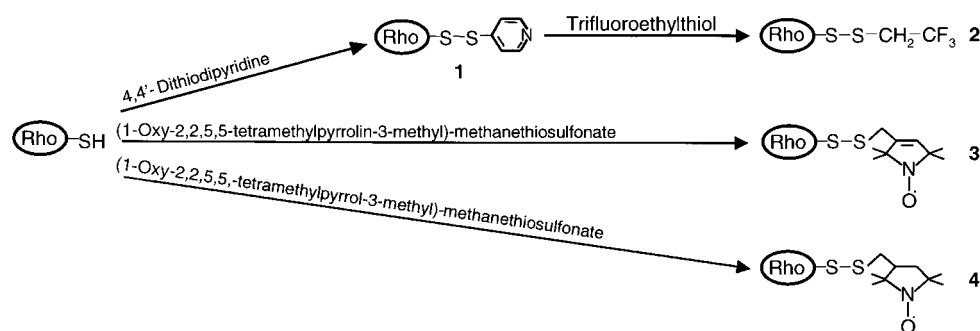


Figure 4. Chemical structures of cysteine derivatives of rhodopsin. Reactions of rhodopsin with 4,4'-dithiodipyridine are described in refs. [9, 40, 41]. The general strategy for disulfide exchange of thiopyridinyl cysteine derivatives of rhodopsin such as **1** with sulfhydryl reagents is described in ref. [9]. The specific application of disulfide exchange with trifluoroethylthiol to form ¹⁹F-labeled derivative **2** is shown in ref. [21]. Use of different thiosulfonate derivatives to form paramagnetic rhodopsin derivatives is illustrated by structures **3** and **4**. The difference between the two labels is described in the text and in ref. [23]. Rho = rhodopsin.

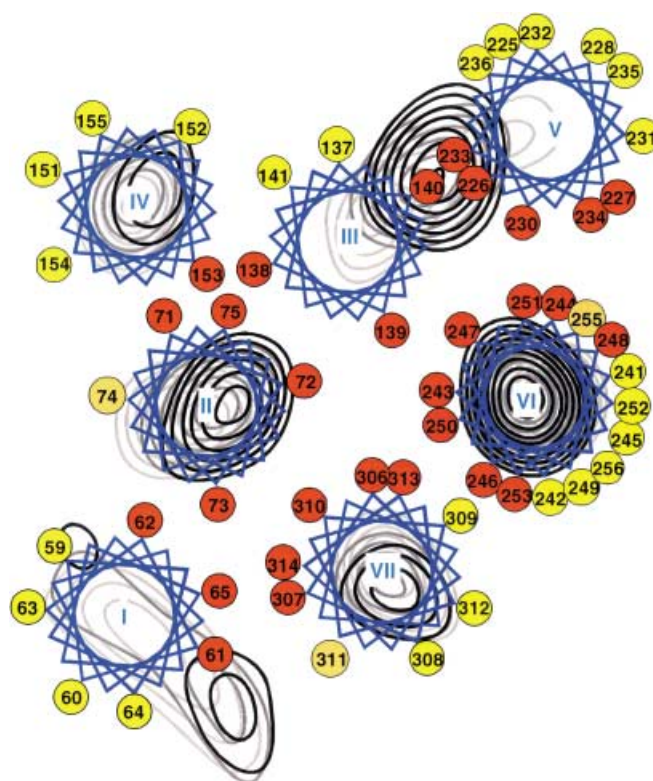


Figure 5. Summary of the results of EPR spectroscopy studies on the mobility of residues at the CP ends of the TM helices.^[6, 7, 20, 24] The figure is a modified version of Figure 5 in ref. [20] but includes the results from all the single-cysteine EPR studies with rhodopsin.^[6, 7, 20, 24] Residue positions in the helical segments are mapped onto electron density contour sections taken at 13, 15, and 17 Å from the center of the membrane.^[42] The map had an effective resolution of 7.5 Å in the membrane plane and 16.5 Å normal to the plane. The circles mark the locations of the α carbon atoms of the residues and are coded on a red to yellow scale according to mobility and accessibility, with red the most immobilized and inaccessible and yellow the most mobile.^[20]

Figure 5, there is a clear pattern in mobility at each helical wheel of the seven TM helices in rhodopsin. Mobile residues are arranged on one side of the wheel, while immobile residues are arranged on the opposite side.^[6, 7, 20, 24] This pattern was used to derive the orientations of the helices based on the hypothesis that immobile residues would face the inside of the helical bundle, while mobile residues face the outside of the helical bundle.^[20] This hypothesis has been verified through comparison of these results with the crystal structure.^[2] Changes in mobility upon light-induced activation have allowed the derivation of a model of rigid-body motion of the helices in rhodopsin.^[6, 8]

4. Rates of Disulfide Bond Formation Qualitatively Indicate Backbone Motion in Dark-State Rhodopsin

Qualitative evidence for motion of dark-state rhodopsin in solution was obtained by study of the rates of disulfide bond formation between cysteine residues placed in the CP domain of rhodopsin.^[10, 11] Disulfide bond formation can be used to establish proximity between amino acids in proteins, a method developed by Falke and Koshland^[25] in studies of the aspartate receptor.^[26, 27] The method is based on structural analysis of disulfide groups in protein crystal structures that have shown preferred conformations for their formation.^[28] The distance between α carbon atoms across the disulfide bond ranges from about 4 to 9 Å in crystal structures, with 95% of all refined disulfide bridges in the range 4.4–6.8 Å long. The average distances across left-handed and right-handed disulfide bonds are 5.88 ± 0.49 Å and 5.07 ± 0.73 Å,^[29] respectively. Thus, the presence of a disulfide bond indicates that the α carbon atoms of the participating cysteine residues are about 5–6 Å apart. However, the geometry derived from crystallography may not hold in solution, especially for mobile regions at protein surfaces.^[29] The formation of a disulfide bond between two cysteine residues does not imply a time-average proximity of the two residues in the protein structure. Once the disulfide bond is formed, the two cysteine residues are locked in a conformation that may not necessarily be favored.

The rates of disulfide bond formation were determined for sets of dicysteine mutants of rhodopsin in which the position of a cysteine residue was kept constant at one site while that of a second cysteine residue was varied within a proximal region.^[10, 11] The rates of disulfide bond formation were measured for different sets of dicysteine mutants (reviewed in ref. [30]). These rates were compared to proximities between amino acids deduced from the crystallographic model.^[2] The reciprocal of the distances obtained as a function of residue position and the rates of disulfide bond formation are reproduced in Figure 6 for disulfide bonds between Cys316 in helix VIII at CL4 and cysteine residues at positions 55–75 in CL1.^[10] The comparison showed excellent correlation between the rates of disulfide bond formation and the interthiol distances derived from the cysteine replacements in the crystal structure. The three positions that most rapidly formed disulfide bonds with Cys316 (H65C, L68C, and V61C) are 4–5 Å distant from Cys316 and positioned facing it. In order for a disulfide bond to form, however, 3–4-Å translational movements would be necessary. This requires that there be sufficient flexibility of the amino acids in this region of the rhodopsin CP face. The fact that only those cysteine residues that faced Cys316 were able to bridge this small gap indicates that there is no unfolding of the ends of the helices, but rather a movement of intact helices to bring residues in CL1 close to Cys316. These results presented the first direct evidence for substantive backbone motion in the CP domain of rhodopsin in solution. The conclusion is supported by the observation by EPR spectroscopy of distributions of distances between spin labels in rhodopsin derivatives.^[14, 31]

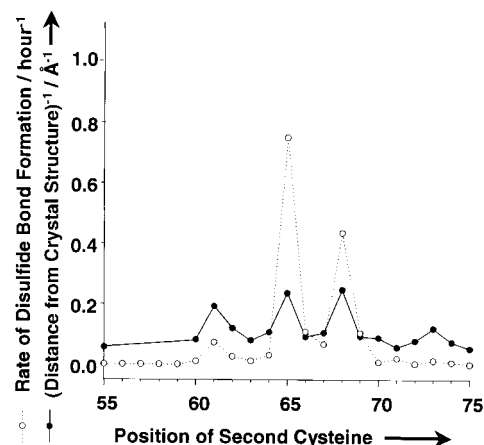


Figure 6. Comparison of rates of disulfide bond formation observed between Cys316 and cysteine residues at positions 55–75 in CL1 (Figure 1) with S–S distances in the rhodopsin crystal structure. (○) Plot of rates of disulfide bond formation in double cysteine mutants Y60C-Y74C/Cys316. Disulfide bond formation was measured at pH 7.7, 25 °C. (●) Reciprocal of distances between S_γ atoms of the two cysteine residues. Distances between sulfur atoms were determined as described in ref. [10].

5. Microsecond to Millisecond Timescale Conformational Fluctuations in the Dark-State Rhodopsin Backbone Revealed by NMR Spectroscopy

Quantitative evidence for conformational fluctuations in rhodopsin came from a solution NMR spectroscopy study of rhodopsin labeled with [α -¹⁵N]lysine.^[32] Despite the presence of 11 lysine residues in rhodopsin, a single sharp signal (signal 1, Figure 7) was obtained in ¹H,¹⁵N HSQC spectra of [α -¹⁵N]lysine rhodopsin under a variety of conditions. Signal 1 was unequivocally assigned to Lys339 in the C-terminal rhodopsin sequence. The signal showed an unusually sharp line-width and a ¹H chemical shift of approximately 8.5 ppm. This observation demonstrated great mobility of the C-terminal peptide sequence

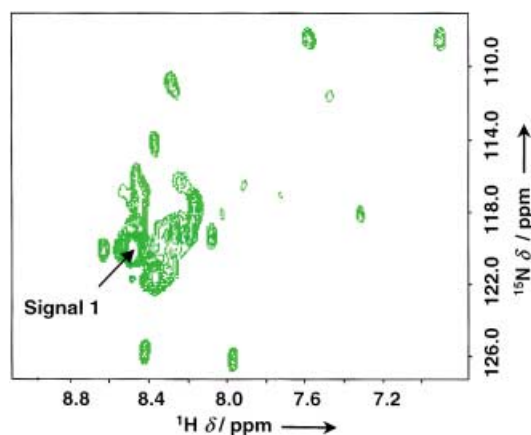


Figure 7. Two-dimensional HSQC spectrum of [α -¹⁵N]lysine rhodopsin.^[32] The spectrum was recorded at 750 MHz at 37 °C. Signal 1 (see text for comments) is indicated by an arrow.

of rhodopsin, a result in agreement with previous evidence; spin labels attached to engineered cysteine residues in the C-terminal sequence exhibit EPR spectra with mobility similar to that of free spin labels in solution.^[33] Further, the amino acids in the C terminus of rhodopsin are hardly visible in the available X-ray diffraction data and have very high B factors^[2] (Figure 2). In addition to the predominant signal 1, a number of further resonances were observed at temperatures above 20 °C that showed a marked variation in intensity (Figure 7) caused by exchange broadening of signals. The heterogeneity in the signal intensity of [α -¹⁵N]lysine resonances is also observed for backbone [α -¹⁵N]tryptophan resonances, but not for side-chain [α -¹⁵N]tryptophan resonances.^[34] These results demonstrate the presence of conformational fluctuations in the backbone of rhodopsin on a microsecond to millisecond timescale while side-chains, in contrast, appear to be more restricted in their conformational dynamics.

6. A Model for the Role of Dark-State Motion in Light-Induced Activation

The conformational fluctuations observed in dark-adapted rhodopsin most likely have functional significance and probably allow light-induced conformational changes that are part of the signaling process to occur. Conformational exchange has also been observed in NMR spectroscopy studies of bacteriorhodopsin, a 7-helical TM protein that undergoes similar light-induced conformational changes to those that occur in rhodopsin.^[35, 36] These results suggest that this behavior may be common for TM helical bundle proteins that undergo functional conformational changes. Fewer fluctuations appear to occur in the side chains of rhodopsin than in the backbone, which suggests that specific side-chain contacts may restrict the rhodopsin dark-state conformation to a "locked" state, without fully restricting motional fluctuations in the helical bundle itself. Thus, it would not be necessary to break and form many specific contacts after retinal isomerization. Rather, a few specific side-chain contacts that restrict the dark state need to be disrupted, while the rest of the backbone of the bundle would easily follow as a result of its high flexibility. This model for a role of specific contacts fits well with previous studies. For example, Trp265 forms a crosslink with retinal in the dark, while no crosslinking occurs in the light.^[12, 13, 37] This observation suggests that there is a side-chain contact between Trp265 and the ionone ring of the retinal. This specific contact is disrupted as a result of light-induced activation. The ionone ring appears to form a new specific side-chain contact after light-induced activation, namely to Ala169.^[13] This conclusion was deduced from the observation that the ionone ring of the retinal crosslinks to Ala169, a residue located more than 10 Å away from the ionone ring in the dark-state crystal structure. Furthermore, Trp161, which is highly conserved and located two helical turns below Ala169, also appears to play a critical role in the light activation process.^[13, 38] The close proximity and similar spatial orientation of Ala169 and Trp161 might indicate that the chromophore forms contacts in order to force protein conformational changes that activate transducin.

The general hypothesis of a conservation of the functional mechanism of signal transduction used by rhodopsin across the entire family of GPCR predicts that any functional role of conformational fluctuations in the resting state of the receptor rhodopsin should be universal for this family of proteins. Indeed, conformational heterogeneity has been observed by single-molecule spectroscopy of the β_2 adrenergic receptor.^[39] At least two distinct substates for the native adrenergic receptor were found. The binding of ligands to the receptor changed the shape of the entire distribution and the populations of the conformational substates. It is an important goal for future GPCR research to quantify the molecular details of the dynamics in different functional states of this class of receptors.

I am grateful to my thesis advisor H. Gobind Khorana for discussions, ideas, support, and training. I would also like to thank the collaborators Ulrike Alexiev, Christian Altenbach, Kewen Cai, John Chung, Elena Getmanova, Wayne L. Hubbell, John Hwa, Michele Loewen, Phil Reeves, Harald Schwalbe, and Peter Wright for their crucial contributions to this work. My PhD studies were supported by a Howard Hughes Predoctoral Fellowship.

- [1] H. G. Khorana, *J. Biomol. Struct. Dyn.* **2000**, *11*, 1–16.
- [2] K. Palczewski, T. Kumasaka, T. Hori, C. A. Behnke, H. Motoshima, B. A. Fox, I. LeTrong, D. C. Teller, T. Okada, R. E. Stenkamp, M. Yamamoto, M. Miyano, *Science* **2000**, *289*, 739–745.
- [3] E. C. Meng, H. R. Bourne, *Trends Pharmacol. Sci.* **2001**, *22*, 587–593.
- [4] T. P. Sakmar, *Curr. Opin. Cell Biol.* **2002**, *14*, 189–195.
- [5] T. Okada, K. Palczewski, *Curr. Opin. Struct. Biol.* **2001**, *11*, 420–426.
- [6] Z. T. Farahbakhsh, K. D. Ridge, H. G. Khorana, W. L. Hubbell, *Biochemistry* **1995**, *34*, 8812–8819.
- [7] C. Altenbach, K. Yang, D. L. Farrens, Z. T. Farahbakhsh, H. G. Khorana, W. L. Hubbell, *Biochemistry* **1996**, *35*, 12470–12478.
- [8] D. L. Farrens, C. Altenbach, K. Yang, W. L. Hubbell, H. G. Khorana, *Science* **1996**, *274*, 768–770.
- [9] J. Klein-Seetharaman, J. Hwa, K. Cai, C. Altenbach, W. L. Hubbell, H. G. Khorana, *Biochemistry* **1999**, *38*, 7938–7944.
- [10] J. Klein-Seetharaman, J. Hwa, K. Cai, C. Altenbach, W. L. Hubbell, H. G. Khorana, *Biochemistry* **2001**, *40*, 12472–12478.
- [11] K. Cai, J. Klein-Seetharaman, C. Altenbach, W. L. Hubbell, H. G. Khorana, *Biochemistry* **2001**, *40*, 12479–12485.
- [12] T. A. Nakayama, H. G. Khorana, *J. Biol. Chem.* **1990**, *265*, 15762–15769.
- [13] B. Borhan, M. L. Souto, H. Imai, Y. Shichida, K. Nakanishi, *Science* **2000**, *288*, 2209–2212.
- [14] C. Altenbach, J. Klein-Seetharaman, K. Cai, H. G. Khorana, W. L. Hubbell, *Biochemistry* **2001**, *40*, 15493–15500.
- [15] C. Altenbach, K. Cai, J. Klein-Seetharaman, H. G. Khorana, W. L. Hubbell, *Biochemistry* **2001**, *40*, 15483–15492.
- [16] K. Takeda, H. Sato, T. Hino, M. Kono, K. Fukuda, I. Sakurai, T. Okada, T. Kouyama, *J. Mol. Biol.* **1998**, *283*, 463–474.
- [17] H. Luecke, B. Schobert, H. T. Richter, J. P. Cartailler, J. K. Lanyi, *J. Mol. Biol.* **1999**, *291*, 899–911.
- [18] H. Luecke, B. Schobert, J. K. Lanyi, E. N. Spudich, J. L. Spudich, *Science* **2001**, *293*, 1499–1503.
- [19] D. R. Grassetti, J. F. Murray, Jr., *Arch. Biochem. Biophys.* **1967**, *119*, 41–49.
- [20] C. Altenbach, J. Klein-Seetharaman, J. Hwa, H. G. Khorana, W. L. Hubbell, *Biochemistry* **1999**, *38*, 7945–7949.
- [21] J. Klein-Seetharaman, E. V. Getmanova, M. C. Loewen, P. J. Reeves, H. G. Khorana, *Proc. Natl. Acad. Sci. USA* **1999**, *96*, 13744–13749.
- [22] J. T. Gerig, *Methods Enzymol.* **1989**, *177*, 3–23.
- [23] H. S. Mchaourab, T. Kalai, K. Hideg, W. L. Hubbell, *Biochemistry* **1999**, *38*, 2947–2955.
- [24] C. Altenbach, K. Cai, H. G. Khorana, W. L. Hubbell, *Biochemistry* **1999**, *38*, 7931–7937.

- [25] J. J. Falke, D. E. J. Koshland, *Science* **1987**, *237*, 1596–1600.
- [26] J. J. Falke, A. F. Dernburg, D. A. Sternberg, N. Zalkin, D. L. Milligan, D. E. J. Koshland, *J. Biol. Chem.* **1988**, *263*, 14850–14858.
- [27] D. L. Milligan, D. E. J. Koshland, *J. Biol. Chem.* **1988**, *263*, 6268–6275.
- [28] J. S. Richardson, *Adv. Protein Chem.* **1981**, *34*, 167–339.
- [29] P. A. Kosen in *Stability of Protein Pharmaceuticals, Part A: Chemical and Physical Pathways of Protein Degradation* (Eds.: T. J. Ahern, M. C. Manning), Plenum Press, New York, **1992**.
- [30] K. Cai, J. Klein-Seetharaman, J. Hwa, W. L. Hubbell, H. G. Khorana, *Biochemistry* **1999**, *38*, 12893–12898.
- [31] C. Altenbach, K.-J. Oh, R. Trabinino, K. Hideg, W. L. Hubbell, *Biochemistry* **2001**, *40*, 15471–15482.
- [32] J. Klein-Seetharaman, P. J. Reeves, M. C. Loewen, E. V. Getmanova, J. Chung, H. Schwalbe, P. E. Wright, H. G. Khorana, *Proc. Natl. Acad. Sci. USA* **2002**, *99*, 3452–3457.
- [33] R. Langen, K. Cai, C. Altenbach, H. G. Khorana, W. L. Hubbell, *Biochemistry* **1999**, *38*, 7918–7924.
- [34] J. Klein-Seetharaman, H. Schwalbe, H. G. Khorana, unpublished results.
- [35] V. Orekhov, K. V. Pervushin, A. S. Arseniev, *Eur. J. Biochem.* **1994**, *219*, 887–896.
- [36] V. Orekhov, G. V. Abdulaeva, L. Musina, A. S. Arseniev, *Eur. J. Biochem.* **1992**, *210*, 223–229.
- [37] T. A. Nakayama, H. G. Khorana, *J. Biol. Chem.* **1991**, *266*, 4269–4275.
- [38] S. W. Lin, T. P. Sakmar, *Biochemistry* **1996**, *35*, 11149–11159.
- [39] G. Peleg, P. Ghanouni, B. K. Kobilka, R. N. Zare, *Proc. Natl. Acad. Sci. USA* **2001**, *98*, 8469–8474.
- [40] Y. S. Chen, W. L. Hubbell, *Membr. Biochem.* **1978**, *1*, 107–130.
- [41] K. Cai, J. Klein-Seetharaman, D. Farrens, C. Zhang, C. Altenbach, W. L. Hubbell, H. G. Khorana, *Biochemistry* **1999**, *38*, 7925–7930.
- [42] V. M. Unger, P. A. Hargrave, J. M. Baldwin, G. F. Schertler, *Nature* **1997**, *389*, 203–206.

Received: May 3, 2002 [M409]